Check for updates

AGU100 ADVANCING EARTH AND SPACE SCIENCE

Geophysical Research Letters

RESEARCH LETTER
10.1002/2018GL076995

Key Points:
- We derive the mean-value theorem for potential fields, the new theoretical basis of the free-air correction, and downward continuation
- We present several formulae for downward continuation based on different numerical solutions of the mean-value theorem for potential fields
- One of the proposed methods has been tested on both synthetic and real cases, and the downward continuation is stable and highly accurate

Supporting Information:
- Supporting Information S1
- Data Set S1
- Data Set S2

Correspondence to:
Q. Lü and J. Yan,
lqt@cags.ac.cn;
yanjy@163.com

Citation:
Zhang, C., Lü, Q., Yan, J., & Qi, G. (2018). Numerical solutions of the mean-value theorem: New methods for downward continuation of potential fields. *Geophysical Research Letters*, *45*, 3461–3470. https://doi.org/10.1002/2018GL076995

Received 2 JAN 2018
Accepted 19 MAR 2018
Accepted article online 26 MAR 2018
Published online 22 APR 2018

Numerical Solutions of the Mean-Value Theorem: New Methods for Downward Continuation of Potential Fields

Chong Zhang[1], Qingtian Lü[1,2], Jiayong Yan[1], and Guang Qi[1]

[1]China Deep Exploration Center (SinoProbe Center), Chinese Academy of Geological Sciences, Beijing, China, [2]Institute of Geophysical and Geochemical Exploration, Chinese Academy of Geological Sciences, Langfang, Hebei, China

Abstract Downward continuation can enhance small-scale sources and improve resolution. Nevertheless, the common methods have disadvantages in obtaining optimal results because of divergence and instability. We derive the mean-value theorem for potential fields, which could be the theoretical basis of some data processing and interpretation. Based on numerical solutions of the mean-value theorem, we present the convergent and stable downward continuation methods by using the first-order vertical derivatives and their upward continuation. By applying one of our methods to both the synthetic and real cases, we show that our method is stable, convergent and accurate. Meanwhile, compared with the fast Fourier transform Taylor series method and the integrated second vertical derivative Taylor series method, our process has very little boundary effect and is still stable in noise. We find that the characters of the fading anomalies emerge properly in our downward continuation with respect to the original fields at the lower heights.

Plain Language Summary A class of novel methods for downward continuation of potential fields are addressed. Because they are new methods and the results are stable, convergent and accurate, and have very little boundary, it is required for rapid publication. The mean-value theorem for potential fields is presented and it shows the vertical variation of potential field simply. The new scientific advance allows convergent and accurate downward continuation because of the different numerical solutions of it. The results improve the anomaly's resolution and enhance the overlapping character. The mean-value theorem and its numerical solutions of potential fields may be the new theoretical basis of the free-air correction and downward continuation.

1. Introduction

The downward continuation of the potential fields can enhance the magnitude of the signal and improve its spatial resolution, so it is useful for extracting the shallower and more subtle sources from the regional anomalies and for studying the mass distributions or geodynamic phenomena below the altitude of the observations (Bouman et al., 2016; Fukao et al., 2001; Hamoudi et al., 1995; Morgan & Blackman, 1993; Sebera et al., 2014). However, downward continuation is a difficult task in potential field data processing and interpretation (Li et al., 2013; Zietz & Bhattacharyya, 1975). The main issues are as follows: First, using the fields of one elevation to obtain the lower ones is divergent and nonharmonic mathematically, which cannot be solved directly (Fedi & Cascone, 2011; Fedi & Florio, 2011; Lieb et al., 2016; Parker, 1977; Xu et al., 2007; Zeng et al., 2013, 2014); second, when downward continuation encounters an exceptional source, oscillation or singularity occurs, which makes the downward continuation unstable (Fedi & Florio, 2002; Nabighian, 1974). Different methods have been proposed to realize the convergent and stable downward continuation in three ways. One is always performed by inverse calculation or finite difference discretization based on the Dirichlet integral formula in the spatial domain (Achache et al., 1987; Bhattacharyya, 1972; Bullard & Cooper, 1948; Ducruix et al., 1974; Henderson, 1970; Mastellone et al., 2013; Morgan & Blackman, 1993). However, the discretized approximation, the multisolutions, the instability calculation and the interpolation estimation are considered in this method (Fedi & Florio, 2002; Ivan, 1994; Leao & Silva, 1989; Novák et al., 2001). Another utilizes the linear multiplicative algorithm based on the convolution in the frequency domain (Dean, 1958; Hughes, 1942; Tomoda & Aki, 1955; Tsuboi & Fuchida, 1937). However, its frequency downward continuation factor should be filtered or regularized to diminish the amplifying impact (Abedi et al., 2013; Clarke, 1969; Ferguson, 1988; Huestis & Parker, 1979; Lima et al., 2013; Pašteka et al., 2012; Pawlowski, 1995; Sebera et al., 2015; Tikhonov et al., 1977; Zhang et al., 2016), and moreover, appropriate methods for extension are necessary (Zhang et al., 2017). The third one is achieved by the Taylor series expansion via the potential fields and their different order derivatives (Ackerman, 1971; Evjen, 1936; Peters, 1949; Trejo, 1954; Zhang et al., 2013), but it needs to address the instability of high-order derivatives (Florio et al., 2006). In addition, because it is a truncated Taylor series expansion, to realize the deep and accurate continuation, multiple-step iterations are needed (Fedi & Florio, 2001; Zhang et al., 2013).

For the unstable and inaccurate problems, we present new downward continuation methods based on numerical solutions of the mean-value theorem (Butcher, 2008; Hairer et al., 1993, 1996) of potential fields. The derivation analysis is performed for the mean-value theorem of potential fields, which could be the theoretical basis of the free-air correction and downward continuation. The mean-value theorem is similar in form to the Taylor series expansion, but they are different in essence. The calculation of the average derivative of the potential fields in the mean-value theorem can be estimated approximately by any practical and effective methods of the numerical solutions. To realize downward continuation, the interval average derivative is approximated by the derivatives at several points, and the upward continuation of the potential fields and its derivatives are computed. Our downward continuation methods can be deduced from a class of the numerical solutions of the mean-value theorem methods. To demonstrate the efficiency, we arbitrarily select one of these methods, the Adams method, to present, and it is applied to the synthetic data and the real case for downward continuation.

2. Theory and Methods

2.1. Mean-Value Theorem for Vertical Variation of Potential Fields

The Taylor series expansion of potential fields, which is applicable to the downward continuation of Laplacian or Newtonian fields, can be expressed as (Fedi & Florio, 2002; Peters, 1949)

$$\begin{aligned} u(x,y,z+h) &\approx \sum_{n=0}^{\infty} \frac{u^{(n)}(x,y,z)}{n!} h^n \\ &= u(x,y,z) + u'(x,y,z)h + \frac{u''(x,y,z)}{2!}h^2 + \dots \\ &\quad + \frac{u^{(n)}(x,y,z)}{n!}h^n + \frac{u^{(n+1)}(x,y,z)}{(n+1)!}h^{(n+1)} + \dots, \end{aligned} \tag{1}$$

where u is the gravity or magnetism fields and h is the distance of continuation. The coordinate system is established with the positive z axis vertically downward throughout section 2.

In the space domain, as the vertical variation of the potential fields is continuously differentiable (Peters, 1949; Roy, 1967), the Taylor formula (not Taylor series) of potential fields is

$$\begin{aligned} u(x,y,z+h) &= u(x,y,z) + u'(x,y,z)h + \frac{u''(x,y,z)}{2!}h^2 + \dots \\ &\quad + \frac{u^{(n)}(x,y,z)}{n!}h^n + \frac{u^{(n+1)}(x,y,\varepsilon)}{(n+1)!}h^{n+1}, \end{aligned} \tag{2}$$

where ε is an indeterminate constant in $[z, z+h]$.

When $n = 1$, formula (1), which is based on the Taylor series expansion, turns into the further approximation as

$$u(x,y,z+h) \approx u(x,y,z) + u'(x,y,z)h. \tag{3}$$

Meanwhile, formula (2) turns into the mean-value theorem formula of potential fields (Wang & Zhu, 2005). The corresponding expression is

$$u(x,y,z+h) = u(x,y,z) + u'(x,y,\varepsilon)h. \tag{4}$$

This is the mean-value theorem for vertical variation of potential fields. Formula (4) can be recognized as the new theoretical basis of potential fields in the free-air correction (Blakely, 1995) instead of the Taylor series expansion. More importantly, it is also the novel theoretical formula of the mean-value theorem downward continuation method.

2.2. Relationship between Downward Continuation by the Taylor Series Expansion and by the Mean-Value Theorem

The convergence radius of formula (1) is $\lim_{n\to\infty}\left|\frac{u^{(n)}(x,y,z)}{n!}\Big/\frac{u^{(n+1)}(x,y,z)}{(n+1)!}\right| = R$. That is, equation (1) holds true only in the convergence interval (with radius R) of the power series expansion of the fields (Hairer et al., 1996). In addition, when $\lim_{n\to\infty}\left(u(x,y,z+h)-\sum_{n=0}^{\infty}\frac{u^{(n)}(x,y,z)}{n!}h^n\right) = 0$, the power series expansion is not only convergent but also equal to u. Otherwise, the power series expansion (1) is convergent but does not hold true (Hairer et al., 1993, 1996). This limits the range of the h value in using the Taylor series expansion. Equation (2) is similar to equation (1), but equation (2) is identical whether the equation $\lim_{n\to\infty}\left(u(x,y,z+h)-\sum_{n=0}^{\infty}\frac{u^{(n)}(x,y,z)}{n!}h^n\right) = 0$ is true or not (Hairer et al., 1993, 1996). Furthermore, although expressions (3) and (4) are similar in form, these two are different in essence. Formula (3) is a truncated Taylor series expansion with a two-order truncation error which is the approximation between the differential of $du = u'(x,y,z)h$ and the difference of $u(x,y,z+h) - u(x,y,z)$ and has to meet the harsh conditions of convergence and equality, whose approximation relation is that equality is only satisfied if h approaches 0. In contrast, formula (4) is an identical equation, which gives the accurate expression of $u(x,y,z+h) - u(x,y,z)$ as the independent variable h is a finite increment but is not infinitely small (Wang & Zhu, 2005).

Although formula (4) has no closed-form solution and cannot be solved directly, we note that the truncated Taylor series expansion from (1) holds only when u is continuously differentiable and h is small enough (Bodvarsson, 1973). Furthermore, the Taylor series expansion involves high-order derivatives as n increase. In practice, the calculation of higher-order vertical derivatives is always unstable (Fedi & Florio, 2002). The mean-value theorem formula only contains the first-order vertical derivatives. For downward continuation, the independent variable z is not infinitesimal and the downward fields need high resolution, which means the mean-value theorem formula (4) is more suitable and efficient.

2.3. Downward Continuation Methods Based On Different Numerical Solutions of the Mean-Value Theorem

Formula (4), which is presented as the theoretical background of downward continuation, has no actual computability. The key problem is how to compute the derivative $u'(\varepsilon)$ practically. It is easy to see that the derivative at an unknown certain point $u'(\varepsilon)$ is equal to the average derivative of the potential fields between the two endpoints from formula (4) (Wang & Zhu, 2005). Therefore, the downward continuation based on formula (4) which contains $u'(\varepsilon)$ can be determined by the approximation methods of the average derivative. Different approximation methods of the average derivative can yield the corresponding algorithms for downward continuation.

If we choose the average derivative to be approximated by the derivative at the point z_0, which is one of the numerical solutions of the mean-value theorem called the Euler scheme in mathematics, we obtain the Euler scheme for the downward continuation:

$$u(x,y,z_0+h) = u(x,y,z_0) + u'(x,y,z_0)h, \tag{5}$$

where "=," which should be "≈," is an assignment, not an equal sign. It is equal to the downward continuation method by the truncated Taylor series expansion with two terms (expression (3)). Since only two terms on the right-hand side of (5) at the point z_0 are used for the approximate calculation, the precision of this downward continuation is relatively low. We deduce further that if we use other numerical solutions of the mean-value theorem to obtain the more accurate approximation of the average derivative through the derivatives at multiple points z_0, $z_0 - h$,…, and $z_0 - (n-1)$h, the precision of downward continuation should be improved. Thus, by using the derivatives and their upward continuation, we could obtain a class of downward continuation methods for potential fields, such as the Runge-Kutta scheme, the Milne format, and the explicit Adams format.

We choose to address the downward continuation by using the explicit Adams method, which is one of the above numerical solutions of the mean-value theorem. We take the integral of equation (4) over the interval $[z_0, z_0 + h]$ based on the Newton-Leibniz formula and obtain

$$u(x, y, z_0 + h) = u(x, y, z_0) + \int_{z_0}^{z_0+h} u'(x, y, \varepsilon)d\varepsilon. \tag{6}$$

On the right-hand side of (6), there is the unknown term $\int_{z_0}^{z_0+h} u'(x, y, \varepsilon)\mathrm{d}\varepsilon$. However, since the first-order vertical derivatives $u'(x, y, z_0 - ih)$ for $i = 0, \ldots, n - 1$ are available by calculation, it can replace the function $u'(x, y, \varepsilon)$ in (6) by Newton's interpolation formula $N_n(x, y, \varepsilon)$ through the point $\{(z_0 - ih, u'(x, y, z_0 - ih))|i = 0, \ldots, n - 1\}$ (Hairer et al., 1993). The numerical analog to (6) is given by

$$u(x, y, z_0 + h) = u(x, y, z_0) + \int_{z_0}^{z_0+h} N_n(x, y, \varepsilon)d\varepsilon. \tag{7}$$

After insertion of the interpolation polynomial, the explicit Adams formula for the downward continuation of potential fields is

$$u(x, y, z_0 + h) = \alpha_0 u(x, y, z_0) + h\begin{pmatrix} \beta_1 u'(x, y, z_0) + \beta_2 u'(x, y, z_0 - h)+ \\ \ldots + \beta_n u'(x, y, z_0 - (n - 1)h) \end{pmatrix}, \tag{8}$$

where the constants $\alpha_0, \beta_1, \beta_2, \ldots\beta_n$ are the coefficients of the Adams methods and can be found in Table 244 on Page 110 of Butcher's (2008) book. The values of these constants and the corresponding truncation errors for the different formulae can also be found in the appropriate books (Butcher, 2008; Hairer et al., 1993, 1996). Classically, the more terms of u' or u that are involved in the calculation, the higher the order the truncation error is. Formulae (5) and (8) are some of the new methods for downward continuation based on numerical solutions of the mean-value theorem which consists of a number of methods.

3. Results

3.1. Downward Continuation of Synthetic Data Example

Consider a three-cuboid source case (Figure 1a). The first cuboid is located at (75, 65, 25) m with an extent of (40, 10, 20) m and contributes the main field anomalies; the second one is smaller than the first one and is located at (65, 90, 22) m with an extent of (10, 20, 20) m; the third cuboid generates the weakest gravity effect and is located at (85, 90, 22) m with an extent of (10, 10, 20) m. The data are 1 m × 1 m in grid point intervals and 150 × 150 in grid measuring point numbers. The density contrast between each of these sources and the surrounding rocks is 0.5 g/cm^3. The positive z axis is vertically upward throughout section 3. For the consistency of comparison, during the calculation, we do not apply any methods to suppress the noise or the high-frequency components, which may include useful information, and we do not extend the area of the gravity anomalies to avoid the boundary effect, which may introduce uncertainties.

The gravity anomalies (Figure 1c) display as if they are one big isolated geological body at the height of $z = 0$ m, but actually, they are dominated by these three bodies individually. At the height of $z = -10$ m, the gravity anomalies (Figure 1d) show the geometry and location of these bodies clearly. The downward continuation results (Figure 1e) are obtained by the fourth-order Adams formula from $z = 0$ m to $z = -10$ m (ten grid intervals of the downward continuation depth). For the downward continuation, the vertical derivatives at $z = 10$ m, $z = 20$ m, and $z = 30$ m are calculated by the upward continuation of the known vertical derivatives at $z = 0$ m. Compared with the model, the shapes of the downward continuation calculated by the fourth-order Adams formula are generally similar to the exact one, which shows that the results of the downward continuation are stable and convergent. The first and second sources are shown individually, but the third one cannot be seen clearly. We increase the order of the Adams formula to eight (Figure 1f) and apply it to the data. The outlines of these three anomalies are presented well and individually by the eighth order. It shows that the higher the order of the Adams formula we use, the more precise result we get, and the downward continuation by the eighth-order Adams formula is stable, convergent and accurate. The small-scale geologic sources are successfully distinguished from the deeper ones by this downward continuation.

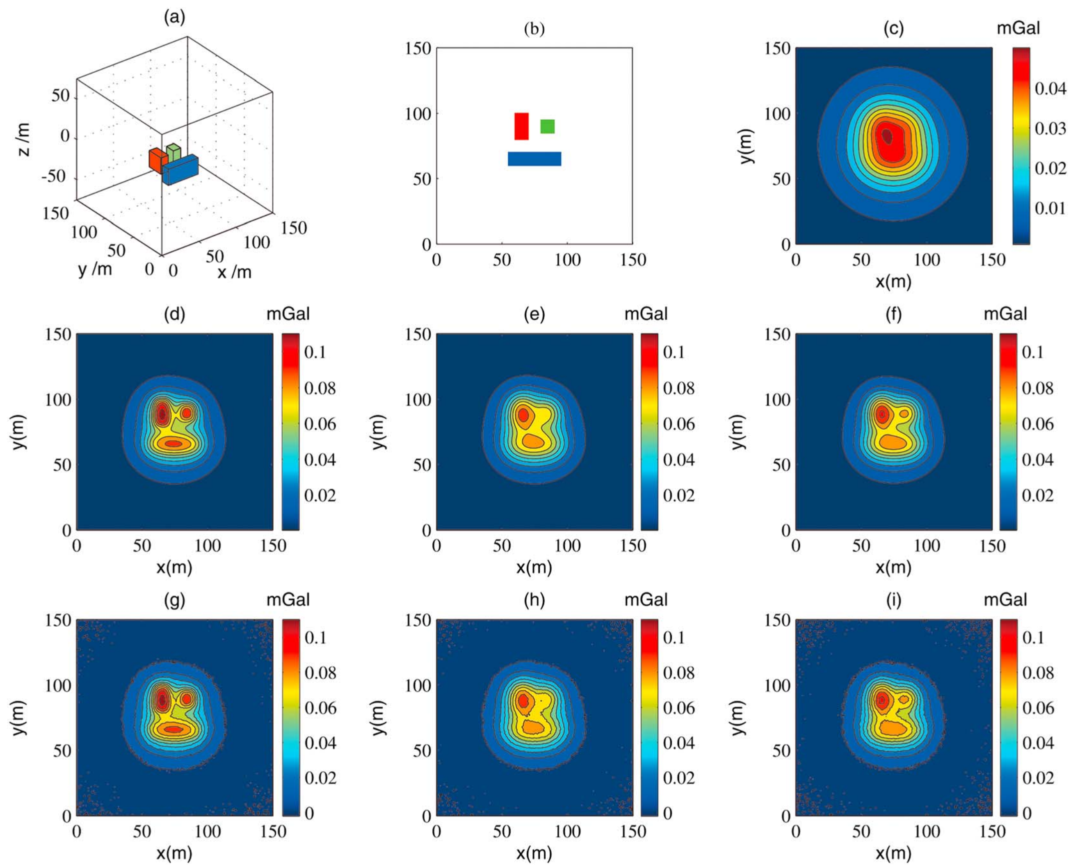

Figure 1. (a) Underground geological bodies, (b) contour map of the geological sources, (c) gravity anomalies at $z = 0$ m, (d) gravity anomalies at $z = -10$ m, (e) downward continuation of (c) by fourth-order Adams formula, (f) downward continuation of (c) by the eighth-order Adams formula, (g) gravity anomalies with 5% noise at $z = -10$ m, (h) downward continuation of (c) by the fourth-order Adams formula, and (i) downward continuation of (c) by the eighth-order Adams formula.

To verify the actual use of our method, we add 5% white noise to the data (Figure 1g). The first-order vertical derivatives we used here with noise are all "known data" which are given by the corresponding formula directly but not calculated from fast Fourier transform (FFT) or other methods. In addition, the leading terms in the downward continuation (8) are the upward continuation of the first-order vertical derivatives. It is known that upward continuation behaves like a low-pass filter which can reduce the noise. Therefore, the downward continuation of the Adams method of numerical solutions of the mean-value theorem (Figures 1h and 1i) is still stable even when noise is contained and is accurate without enhancing the noise too much.

For comparison, the downward continuation methods, which are the Taylor series expansion with vertical derivatives (higher than first order) calculated by FFT (FFT Taylor series), the Taylor series expansion with vertical derivatives calculated by ISVD (ISVD Taylor series) which is the abbreviation of the integrated second vertical derivative method proposed by Fedi & Florio, 2001, and one of the numerical solutions of the mean-value theorem (the Adams formula), are applied to the synthetic data. The number of the summation terms in each of these three methods is nine. We obtain the downward continuation of the noise-free data by these three methods from $z = 0$ m to $z = -3$ m (three grid intervals). Compared with the theoretical anomaly (Figure 2a) at $z = -3$ m, the FFT Taylor series method (Figure 2b) does not match well with the theoretical one and has strong boundary effect; the ISVD Taylor series method (Figure 2c) shows a stable result but has some differences from the theoretical one, and our method (Figure 2d) gives a stable and accurate result and has only weak boundary effect. The corresponding residual errors of these three methods are smaller and smaller from the FFT Taylor series to our method and (Figures 2f to 2h) and show similar proofs with the above downward continuation. To simulate realistic cases, the anomaly is corrupted with 5% white noise (Figure 2i). The downward

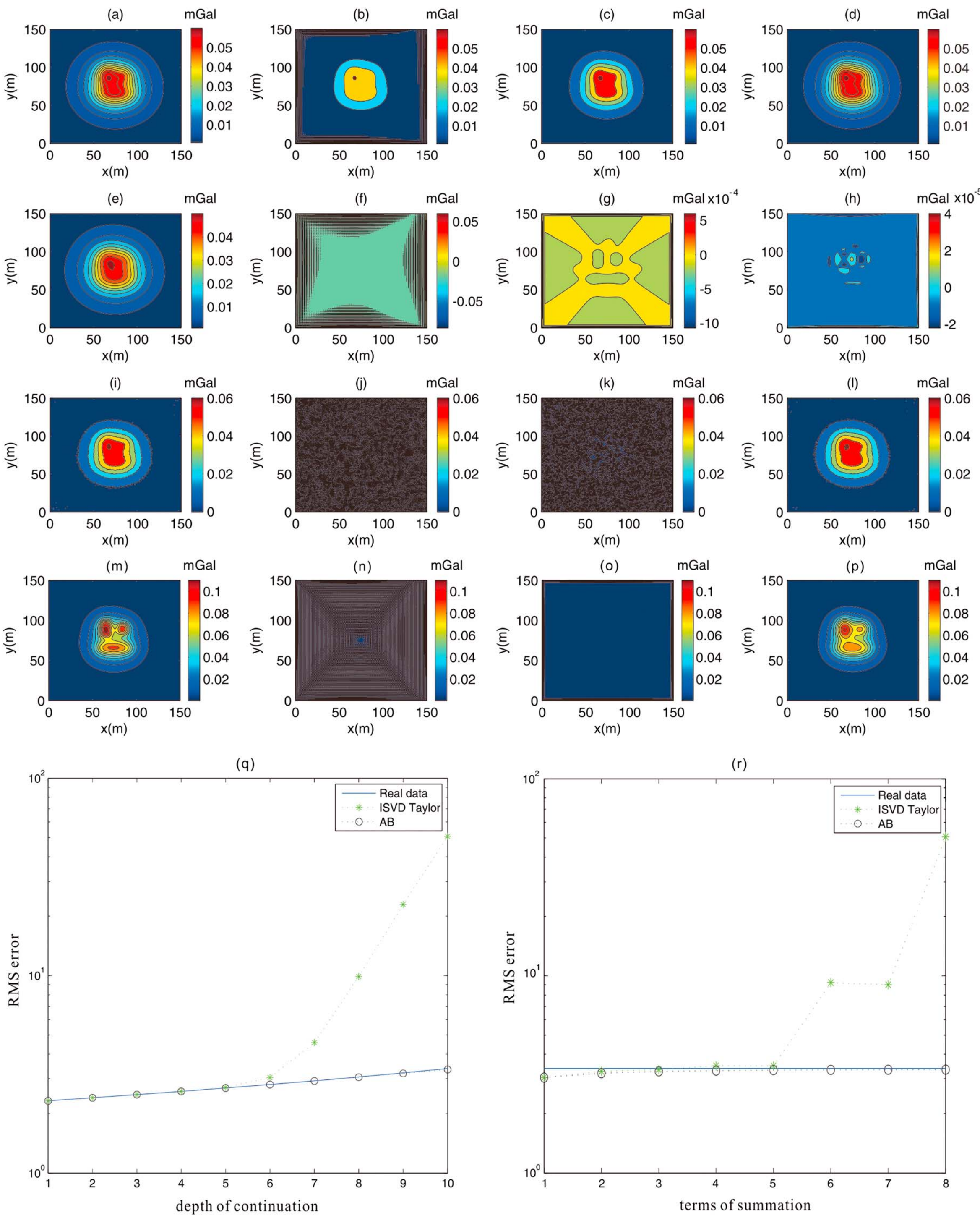

Figure 2. (a) Gravity anomalies at $z = -3$ m, (b) downward continuation by the FFT Taylor series method to $z = -3$ m, (c) downward continuation by the integrated second vertical derivative (ISVD) Taylor series method to $z = -3$ m, (d) downward continuation by the eighth-order Adams formula to $z = -3$ m, (e) gravity anomalies at $z = 0$ m, (f) residual error between (a) and (b), (g) residual error between (a) and (c), (h) residual error between (a) and (d), (i) gravity anomalies at $z = -3$ m with 5% white noise, (j) downward continuation by the fast Fourier transform FFT Taylor series method with 5% white noise to $z = -3$ m, (k) downward continuation by the ISVD Taylor series method with 5% white noise to $z = -3$ m, (l) downward continuation by the eighth-order Adams formula with 5% white noise to $z = -3$ m, (m) gravity anomalies at $z = -8$ m, (n) downward continuation by the fast Fourier transform Taylor series method to $z = -8$ m, (o) downward continuation by the ISVD Taylor series method to $z = -8$ m, (p) downward continuation by the eighth-order Adams formula to $z = -8$ m. (q) Root-mean-square errors of the synthetic data, the downward continuation by the series, the downward continuation by the Adams formula with the increasing of continuation depth, and (r) root-mean-square errors of the synthetic data, the downward continuation of 10 m by the Taylor series, the downward continuation of 10 m by the Adams formula with the increasing of the number of summation terms.

10.1002/2018GL076995

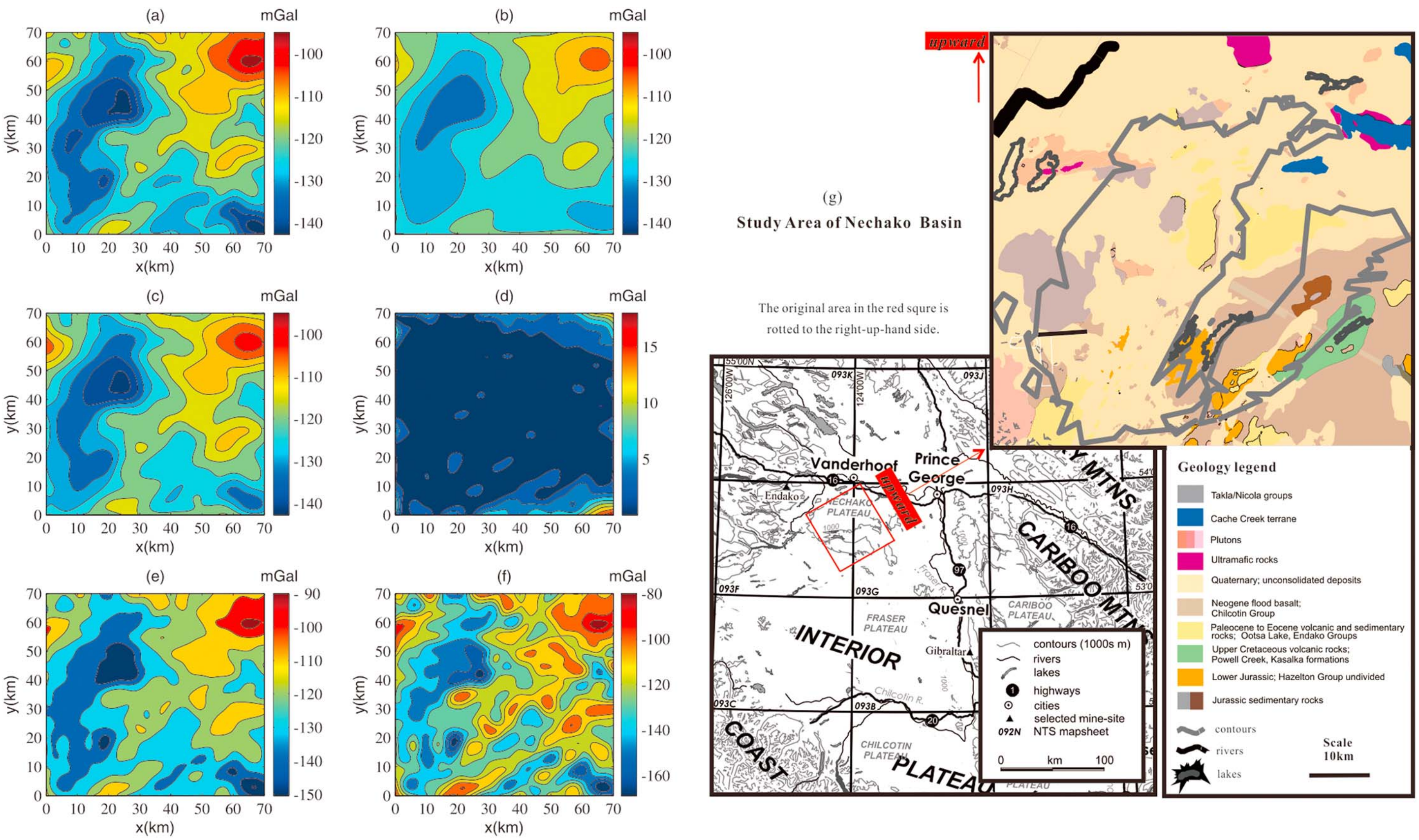

Figure 3. (a) Bouguer gravity anomalies of Nechako Basin, (b) upward continuation of the Bouguer gravity anomalies to $z = 4$ km, (c) downward continuation of (b) to $z = 0$ km by this method, (d) residual error between real gravity anomalies (a) and downward continuation (c), (e) downward continuation of (a) to $z = -1.2$ km by this method, (f) downward continuation of (a) to $z = -2.8$ km by this method. (g) Geology of the Nechako Basin.

continuation by the FFT Taylor series (Figure 2j) and the ISVD Taylor series (Figure 2k) are not convergent with the depth of three intervals, but our method (Figure 2l) is still stable, which indicates that our method is especially more useful than the other two methods in the cases where the data are corrupted by noise.

Increasing the depth of the downward continuation, we obtain the results from $z = 0$ m to $z = -8$ m. The downward continuation of the noise-free data is divergent by the FFT Taylor series (Figure 2n) and the ISVD Taylor series (Figure 2o), while our method (Figure 2p) is convergent and stable, which demonstrates that our method is efficient for deeper downward continuation than the other two methods. Compared with the theoretical anomaly (Figure 2m) at the depth of eight intervals, our method still shows good correspondence with it.

To further evaluate our method, we compare the root-mean-square (RMS) errors of the ISVD Taylor series method with the RMS errors of our method (the Adams formula). By fixing the number of the summation terms, we increase the downward continuation depth, and by fixing the downward continuation depth, we increase the summation number. The RMS errors (Figure 2q) show that the ISVD Taylor series method exceeds the theoretical value at the depth of $z = -6$ m (six grid intervals) and our method fits well with the theoretical one, which means that the downward continuation depth of the ISVD Taylor series method is limited to the prededuction and that of our method is larger. As the depth of downward continuation is fixed, the RMS error of the ISVD Taylor series method diverges at six summation terms but our method is still convergent (Figure 2r). This difference might be caused by the instability of the calculation of high-order vertical derivatives, and this indicates that our method is more convergent and stable.

3.2. Downward Continuation of Nechako Basin Airborne Gravity Data

To further verify the actual efficiency, we apply the eighth-order Adams of the numerical solutions of the mean-value theorem to the airborne Bouguer gravity anomaly (Figure 3a) of Nechako Basin in Canada. The data are 0.4 km × 0.4 km in grid point intervals and 179 × 179 in grid measuring point numbers. We do an upward continuation of the gravity anomaly to $z = 4$ km (ten grid intervals), shown in Figure 3b. For comparison (Caress & Parker, 1989), let the gravity anomaly in Figure 3b and the Bouguer gravity anomaly in Figure 3a be the upper field and the lower field, respectively. The downward continuation of Figure 3b to ten grid intervals by our method is shown in Figure 3c. The result (Figure 3c) is stable and fits well with the real data. It also shows some small-scale information that does not exist in the prior downward continuation anomaly (Figure 3b), but it is consistent with the original measured gravity anomaly (Figure 3a), which strengthens the effect of downward continuation's advantages and indicates the accuracy of our method. The residual error (Figure 3d) between the original gravity anomaly at the lower altitude and the downward continuation result is small, which confirms the reliability and advantage of our method.

Following the above verification, we do downward continuation directly with the measured gravity anomaly (Figure 3a) to three grid intervals (Figure 3e) and seven grid intervals (Figure 3f) by our method. The result of three grid intervals is almost the same as the original predownward anomaly, but it amplifies the range of the anomaly. Deeper to seven grid intervals, the small-scale anomalies and the structure distributions are more obvious and better displayed. The two NE-SW direction structural lines in the southeastern part are presented, and the high and low anomalies mixed up together in the northwest central part are separated. These structural characters are coincident with the contours of the rock distributions in Figure 3g, which are adapted from the geology by Riddell (2011) and Andrews et al. (2011).

4. Conclusions

We theoretically give the mean-value theorem for vertical variation of potential fields, which could be the theoretical basis of some data processing and interpretation methods. Based on numerical solutions of the mean-value theorem, we present a class of novel methods for downward continuation with the advantage of the first-order vertical derivatives and their upward continuation. Compared with the Taylor series expansion, the analysis reveals that our methods do not presuppose the limit of the radius of convergence and do not need to compute the unstable high-order derivatives. In addition, our methods avoid a huge amount of calculation and involve very little of the high-frequency oscillations which are increasing with depth. An arbitrarily selected method (the Adams formula method) of ours is discussed to simplify the presentation and is tested on the synthetic data and on a real case to yield convergent and stable downward continuation. The results reveal that our method is efficient to enhance the useful signal and is accurate to delineate and sharpen the anomalies including the small-scale bodies and the overlapping characters. Our method has deep continuation depth and very little in the way of boundary effect. Even for the system with noise, the proposed method is useful and the result is still stable. In future research, the mean-value theorem for potential fields should be developed further to other aspects. The details of different numerical solutions of the mean-value theorem downward continuation should be derived and discussed. To obtain the optimal method, the advantages and disadvantages of these kinds of methods should be compared.

Acknowledgments

The authors would like to thank Danian Huang, Kai Zhang and Pengbo Qin for their discussions about this manuscript. The authors gratefully acknowledge Yaoguo Li and an anonymous reviewer for their constructive comments and thank Monika Korte for the editing of Geophysical Research Letters. The authors also thank Natural Resources Canada for providing the real data over Canada, which will be available at http://www.nrcan.gc.ca/. The synthetic data supporting this article are provided in the supporting information (Table S1). This work was supported by the National Key R&D Program of China (2016YFC0600201 and 2016YFC0600101), the National Natural Science Foundation of China (41630320 and 41574133), the China Geological Survey Project (DD20179611 and DD20160082) and the Basic Scientific Research Funds of the Chinese Academy of Geological Sciences (JYYWF20180101).

References

Abedi, M., Gholami, A., & Norouzi, G. H. (2013). A stable downward continuation of airborne magnetic data: A case study for mineral prospectivity mapping in central Iran. *Computers & Geosciences*, *52*(1), 269–280. https://doi.org/10.1016/j.cageo.2012.11.006

Achache, J., Abtout, A., & Le Mouël, J. L. (1987). The downward continuation of Magsat crustal anomaly field over Southeast Asia. *Journal of Geophysical Research*, *92*(B11), 11,584–11,596. https://doi.org/10.1029/JB092iB11p11584

Ackerman, J. (1971). Downward continuation using the measured vertical gradient. *Geophysics*, *36*(3), 609–612. https://doi.org/10.1190/1.1440196

Andrews, G. D., Plouffe, A., Ferbey, T., Russell, J. K., Brown, S. R., & Anderson, R. G. (2011). The thickness of Neogene and Quaternary cover across the central Interior Plateau, British Columbia: Analysis of water-well drill records and implications for mineral exploration potential[12]. *Canadian Journal of Earth Sciences*, *48*(6), 973–986. https://doi.org/10.1139/e10-080

Bhattacharyya, B. K. (1972). Design of spatial filters and their application to high-resolution aeromagnetic data. *Geophysics*, *37*(1), 68–91. https://doi.org/10.1190/1.1440253

Blakely, R. J. (1995). *Potential theory in gravity and magnetic applications*. Cambridge, UK: Cambridge University Press. https://doi.org/10.1017/CBO9780511549816

Bodvarsson, G. (1973). Downward continuation of constrained potential fields. *Journal of Geophysical Research*, *78*(8), 1288–1292. https://doi.org/10.1029/JB078i008p01288

Bouman, J., Ebbing, J., Fuchs, M., Sebera, J., Lieb, V., Szwillus, W., et al. (2016). Satellite gravity gradient grids for geophysics. *Scientific Reports*, *6*(1), 21050. https://doi.org/10.1038/srep21050

Bullard, E., & Cooper, R. (1948). The determination of the masses necessary to produce a given gravitational field. *Proceedings of the Royal Society of London. Series A: Mathematical and Physical Sciences*, *194*(1038), 332–347. https://doi.org/10.1098/rspa.1948.0084

Butcher, J. C. (2008). *Numerical methods for ordinary differential equations*. Chichester, UK: John Wiley & Sons. https://doi.org/10.1002/9780470753767

Caress, D. W., & Parker, R. L. (1989). Spectral interpolation and downward continuation of marine magnetic anomaly data. *Journal of Geophysical Research*, *94*(B12), 17,393–17,407. https://doi.org/10.1029/JB094iB12p17393

Clarke, G. K. C. (1969). Optimum second-derivative and downward-continuation filters. *Geophysics*, *34*(3), 424–437. https://doi.org/10.1190/1.1440020

Dean, W. C. (1958). Frequency analysis for gravity and magnetic interpretation. *Geophysics*, *23*(1), 97–127. https://doi.org/10.1190/1.1438457

Ducruix, J., Le, M. J. L., & Courtillot, V. (1974). Continuation of three-dimensional potential fields measured on an uneven surface. *Geophysical Journal International*, *38*(2), 299–314. https://doi.org/10.1111/j.1365-246X.1974.tb04122.x

Evjen, H. M. (1936). The place of the vertical gradient in gravitational interpretations. *Geophysics*, *1*(1), 127–136. https://doi.org/10.1190/1.1437067

Fedi, M., & Cascone, L. (2011). Composite continuous wavelet transform of potential fields with different choices of analyzing wavelets. *Journal of Geophysical Research*, *116*, B07104. https://doi.org/10.1029/2010JB007882

Fedi, M., & Florio, G. (2001). Detection of potential fields source boundaries by enhanced horizontal derivative method. *Geophysical Prospecting*, *49*(1), 40–58. https://doi.org/10.1046/j.1365-2478.2001.00235.x

Fedi, M., & Florio, G. (2002). A stable downward continuation by using the ISVD method. *Geophysical Journal International*, *151*(1), 146–156. https://doi.org/10.1046/j.1365-246X.2002.01767.x

Fedi, M., & Florio, G. (2011). Normalized downward continuation of potential fields within the quasi-harmonic region. *Geophysical Prospecting*, *59*(6), 1087–1100. https://doi.org/10.1111/j.1365-2478.2011.01002.x

Ferguson, J. F. (1988). Models of the Bouguer gravity and geologic structure at Yucca Flat, Nevada. *Geophysics*, *53*(2), 231–244. https://doi.org/10.1190/1.1442458

Florio, G., Fedi, M., & Pasteka, R. (2006). On the application of Euler deconvolution to the analytic signal. *Geophysics*, *71*(6), L87–L93. https://doi.org/10.1190/1.2360204

Fukao, Y., Widiyantoro, S., & Obayashi, M. (2001). Stagnant slabs in the upper and lower mantle transition region. *Reviews of Geophysics*, *39*(3), 291–323. https://doi.org/10.1029/1999RG000068

Hairer, E., Norsett, S. P., & Wanner, G. (1993). *Solving ordinary differential equations I: Nonstiff problems*. Berlin, Heidelberg: Springer-Verlag.

Hairer, E., Norsett, S. P., & Wanner, G. (1996). *Solving ordinary differential equations II: Stiff and differential algebraic problems*. Berlin, Heidelberg: Springer-Verlag. https://doi.org/10.1007/978-3-642-05221-7

Hamoudi, M., Achache, J., & Cohen, Y. (1995). Global Magsat anomaly maps at ground level. *Earth and Planetary Science Letters*, *133*(3–4), 533–547. https://doi.org/10.1016/0012-821X(95)00036-C

Henderson, R. G. (1970). On the validity of the use of the upward continuation integral for total magnetic intensity data. *Geophysics*, *35*(5), 916–919. https://doi.org/10.1190/1.1440137

Huestis, S. P., & Parker, R. L. (1979). Upward and downward continuation as inverse problems. *Geophysical Journal International*, *57*(1), 171–188. https://doi.org/10.1111/j.1365-246X.1979.tb03779.x

Hughes, D. S. (1942). The analytic basis of gravity interpretation. *Geophysics*, *7*(2), 169–178. https://doi.org/10.1190/1.1445004

Ivan, M. (1994). Upward continuation of potential fields from a polyhedral surface 1. *Geophysical Prospecting*, *42*(5), 391–404. https://doi.org/10.1111/j.1365-2478.1994.tb00217.x

Leao, J. W., & Silva, J. B. (1989). Discrete linear transformations of potential field data. *Geophysics*, *54*(4), 497–507. https://doi.org/10.1190/1.1442676

Li, Y., Devriese, S. G. R., Krahenbuhl, R. A., & Davis, K. (2013). Enhancement of magnetic data by stable downward continuation for UXO application. *IEEE Transactions on Geoscience and Remote Sensing*, *51*(6), 3605–3614. https://doi.org/10.1109/TGRS.2012.2220146

Lieb, V., Schmidt, M., Dettmering, D., & Börger, K. (2016). Combination of various observation techniques for regional modeling of the gravity field. *Journal of Geophysical Research: Solid Earth*, *121*, 3825–3845. https://doi.org/10.1002/2015JB012586

Lima, E. A., Weiss, B. P., Baratchart, L., Hardin, D. P., & Saff, E. B. (2013). Fast inversion of magnetic field maps of unidirectional planar geological magnetization. *Journal of Geophysical Research: Solid Earth*, *118*, 2723–2752. https://doi.org/10.1002/jgrb.50229

Mastellone, D., Fedi, M., Ialongo, S., & Paoletti, V. (2013). Volume Continuation of potential fields from the minimum-length solution: An optimal tool for continuation through general surfaces. *Seg Meeting*, *111*, 346–355.

Morgan, J. P., & Blackman, D. K. (1993). Inversion of combined gravity and bathymetry data for crustal structure: A prescription for downward continuation. *Earth and Planetary Science Letters*, *119*(1–2), 167–179. https://doi.org/10.1016/0012-821X(93)90014-Z

Nabighian, M. N. (1974). Additional comments on the analytic signal of two-dimensional magnetic bodies with polygonal cross-section. *Geophysics*, *39*(1), 85–92. https://doi.org/10.1190/1.1440416

Novák, P., Kern, M., & Schwarz, K. P. (2001). Numerical studies on the harmonic downward continuation of band-limited airborne gravity. *Studia Geophysica et Geodaetica*, *45*(4), 327–345. https://doi.org/10.1023/A:1022028218964

Parker, R. L. (1977). Understanding inverse theory. *Annual Review of Earth and Planetary Sciences*, *5*(1), 35–64. https://doi.org/10.1146/annurev.ea.05.050177.000343

Pašteka, R., Karcol, R., Kušnirák, D., & Mojzeš, A. (2012). REGCONT: A Matlab based program for stable downward continuation of geophysical potential fields using Tikhonov regularization. *Computers & Geosciences*, *49*(4), 278–289. https://doi.org/10.1016/j.cageo.2012.06.010

Pawlowski, R. S. (1995). Preferential continuation for potential-field anomaly enhancement. *Geophysics*, *60*(2), 390–398. https://doi.org/10.1190/1.1443775

Peters, L. J. (1949). The direct approach to magnetic interpretation and its practical application. *Geophysics*, *14*(3), 290–320. https://doi.org/10.1190/1.1437537

Riddell, J. (2011). Lithostratigraphic and tectonic framework of Jurassic and Cretaceous Intermontane sedimentary basins of south-central British Columbia[1]. *Canadian Journal of Earth Sciences*, *48*(6), 870–896. https://doi.org/10.1139/e11-034

Roy, A. (1967). Convergence in downward continuation for some simple geometries. *Geophysics*, *32*(5), 853–866. https://doi.org/10.1190/1.1439894

Sebera, J., Pitoňák, M., Hamáčková, E., & Novák, P. (2015). Comparative study of the spherical downward continuation. *Surveys in Geophysics*, *36*(2), 253–267. https://doi.org/10.1007/s10712-014-9312-0

Sebera, J., Šprlák, M., Novák, P., Bezděk, A., & Valľko, M. (2014). Iterative spherical downward continuation applied to magnetic and gravitational data from satellite. *Surveys in Geophysics*, *35*(4), 941–958. https://doi.org/10.1007/s10712-014-9285-z

Tikhonov, A. N., Arsenin, V. I., & John, F. (1977). *Solutions of ill-posed problems* (Vol. 14). Washington, DC: Winston.

Tomoda, Y., & Aki, K. (1955). Use of the function sin *x/x* in gravity problems. *Proceedings of the Japan Academy*, *31*(7), 443–448.

Trejo, C. A. (1954). A note on downward continuation of gravity. *Geophysics*, *19*(1), 71–75. https://doi.org/10.1190/1.1437972

10.1002/2018GL076995

Tsuboi, C., & Fuchida, T. (1937). Relation between gravity anomalies and corresponding sub-terranean mass distribution, 1. *Bulletin of the Earthquake Research Institute, Tokyo University*, *15*, 636–649.

Wang, X. M., & Zhu, H. L. (2005). *Calculation method* (in Chinese). Beijing: High Education Press.

Xu, S. Z., Yang, J., Yang, C., Xiao, P., Chen, S., & Guo, Z. (2007). The iteration method for downward continuation of a potential field from a horizontal plane. *Geophysical Prospecting*, *55*(6), 883–889. https://doi.org/10.1111/j.1365-2478.2007.00634.x

Zeng, X., Li, X., Su, J., Liu, D., & Zou, H. (2013). An adaptive iterative method for downward continuation of potential-field data from a horizontal plane. *Geophysics*, *78*(4), 43–J52. https://doi.org/10.1190/geo2012-0404.1

Zeng, X., Liu, D., Li, X., Chen, D., & Niu, C. (2014). An improved regularized downward continuation of potential field data. *Journal of Applied Geophysics*, *106*(7), 114–118. https://doi.org/10.1016/j.jappgeo.2014.04.015

Zhang, C., Huang, D., & Liu, J. (2017). Milne method for downward continuation of gravity field. *Chinese Journal of Geophysics*, *60*(11), 4212–4220. https://doi.org/10.6038/cjg20171109

Zhang, H., Ravat, D., & Hu, X. (2013). An improved and stable downward continuation of potential field data: The truncated Taylor series iterative downward continuation method. *Geophysics*, *78*(5), J75–J86. https://doi.org/10.1190/geo2012-0463.1

Zhang, Y., Wong, Y. S., & Lin, Y. (2016). BTTB–RRCG method for downward continuation of potential field data. *Journal of Applied Geophysics*, *126*, 74–86. https://doi.org/10.1016/j.jappgeo.2016.01.009

Zietz, I., & Bhattacharyya, B. K. (1975). Magnetic anomalies over the continents and their analyses. *Reviews of Geophysics*, *13*(3), 176–179. https://doi.org/10.1029/RG013i003p00176